



RESEARCH ARTICLE OPEN ACCESS

Self-Adaptive, Untethered Soft Gripper System for Efficient Agricultural Harvesting

Yunwei Zhao¹ | Wenwei Zhao¹ | Maozheng Song¹ | Yi Jin² | Zheng Liu¹ | Md Shariful Islam²  | Xiaomin Liu¹ | Changyong (Chase) Cao^{2,3,4} 

¹School of Mechanical Engineering, Beihua University, Jilin, China | ²Department of Mechanical and Aerospace Engineering, Case Western Reserve University, Cleveland, Ohio, USA | ³Department of Electrical, Computer, and Systems Engineering, Case Western Reserve University, Cleveland, Ohio, USA | ⁴Department of Civil and Environmental Engineering, Case Western Reserve University, Cleveland, Ohio, USA

Correspondence: Xiaomin Liu (xiaomin_liu@beihua.edu.cn) | Changyong (Chase) Cao (ccao@case.edu)

Received: 18 June 2024 | **Revised:** 25 April 2025 | **Accepted:** 7 June 2025

Funding: financial support from the Department of Science and Technology of Jilin Province, China (YDZJ202401396ZYTS, YDZJ202201ZYTS624). Yi Jin, Md Shariful Islam, and C. Chase Cao are grateful for the support from National Science Foundation (ECCS-2024649), USDA-NIFA (Grant No. 2021-67021-42113), and Case Western Reserve University.

Keywords: self-adaptive grasping | smart grippers | soft pneumatic actuators | soft robots | untethered robots

ABSTRACT

As modern agriculture faces increasing demands for efficiency and automation, this study presents a novel, untethered soft gripper system designed for autonomous and efficient harvesting. At the core of this innovation is a piston-driven, pneumatically actuated gripper embedded with flexible tactile sensors, enabling operation without an external air source. The system integrates a compact motorized syringe, forming a closed-loop fluid circuit that provides precise pressure control for adaptive grasping. The pneumatic actuation mechanism regulates air pressure from -30 to 180 kPa, allowing the gripper to perform delicate and adaptive handling, particularly suited for tree fruits and other fragile crops. A key feature of the system is its intelligent control mechanism, which seamlessly combines pneumatic and electrical systems to enhance autonomy and versatility in agricultural applications. The integration of size recognition and adaptive grasping, enabled by force feedback from embedded tactile sensors, ensures safe, efficient, and damage-free harvesting. Demonstrating exceptional potential for autonomous agricultural operations, the untethered soft gripper system offers enhanced independence, maneuverability, and adaptability across diverse harvesting environments. Its ability to optimize crop handling while minimizing damage highlights its significance as a pioneering solution for the future of automated agriculture.

1 | Introduction

As agricultural labor shortages become more pronounced, research in robotic harvesting technology has surged to address the growing need for automation in agriculture (Tinoco 2021a; Bac et al. 2014; Morar et al. 2020). A primary challenge in this field is the development of robotic systems capable of safely and adaptively picking fruits and vegetables without causing damage (Hemming et al. 2016; Silwal et al. 2017; Hughes et al. 2016). These challenges stem from various factors,

including the variability of outdoor environments, inconsistencies in fruit shape and size, and the delicate nature of produce. Furthermore, harvesting robots must strike a balance between versatility, programmability, and cost-efficiency to be viable for large-scale agricultural use.

Harvesting robots typically consist of four key components: a visual system, a control system, a mobility device, and a manipulator, which includes both the mechanical arm and the end effector (Jia et al. 2020; Feng 2021; Davidson et al. 2020;

This is an open access article under the terms of the [Creative Commons Attribution](https://creativecommons.org/licenses/by/4.0/) License, which permits use, distribution and reproduction in any medium, provided the original work is properly cited.

© 2025 The Author(s). *Journal of Field Robotics* published by Wiley Periodicals LLC.

Navas 2021a; Silwal et al. 2017). Among these, the end effector plays a crucial role, as it directly interacts with the fruit, determining the system's overall efficiency and effectiveness. The design of the end effector must consider factors such as grasping force, flexibility, dexterity, and sensing capabilities to meet the specific manipulation requirements of different crops. Recent research has explored various end-effector designs to improve agricultural harvesting performance (Vrochidou et al. 2022; Goulart et al. 2023; Elfferich et al. 2022; Tinoco 2021b).

Grippers are the most commonly used type of end effector in fruit-harvesting robots (Bechar and Vigneault 2016). Traditional grippers, often designed with rigid structures for heavy loads and precision tasks, lack the adaptability required for handling fruits of different sizes, shapes, and textures (Goulart et al. 2023; Blanes et al. 2011; Zhang 2020a, 2020b). In contrast, soft grippers, made from compliant and flexible materials, provide greater versatility and reduce the risk of damaging fruits and vegetables (Hughes et al. 2016; Navas 2021a; Elfferich et al. 2022). Soft grippers can be actuated using various mechanisms, including tendon-driven systems (Chen et al. 2020), soft active materials (Wang and Ahn 2017; Li et al. 2019; Cao and Zhao 2013), and pneumatic or hydraulic systems (Liu et al. 2021, 2022; Chen et al. 2023). Among these, soft pneumatic grippers are particularly attractive due to their simplicity, robustness, and cost-effectiveness (Shintake et al. 2018; Navas 2021b; Karimi et al. 2022).

Several recent studies have contributed to advancements in soft pneumatic grippers for agricultural applications. For example, Bell et al. developed an untethered flexible pneumatic actuator powered by a peristaltic pump, though its efficiency was relatively low (Bell et al. 2021). Similarly, Li et al. designed a bio-inspired winding-based gripper, but its single-action solenoid valve system limited its dexterity and adaptability (Li et al. 2021). Despite these advancements, soft robotic sensing and intelligence remain emerging research areas. Conventional sensors are often too rigid or inflexible to be integrated into soft robotic systems, as they lack compliance and extensibility under large deformations. To address this, researchers have developed stretchable and flexible sensors that can be embedded into soft robotic structures (Rogers et al. 2010; Li et al. 2017; Chen et al. 2018). These bioinspired sensors, modeled after human skin, can detect a range of environmental stimuli, including contact forces, hardness, temperature, and position (Yamaguchi et al. 2019; Chen et al. 2022; Dahiya et al. 2019). The integration of sensing technology significantly improves the adaptability and functionality of soft grippers, enabling more realistic and intelligent robotic manipulation in agricultural applications.

Building on recent advancements in robotic harvesting technology, this study aims to develop and evaluate a cost-effective, untethered, piston-driven, pneumatically actuated adaptive soft gripper system equipped with flexible tactile sensors. The untethered soft gripper system employs a piston-driven pneumatic actuation method, offering a streamlined and compact alternative to conventional pump-and-valve systems. By directly connecting the adaptive soft gripper to the piston, the system eliminates the need for multiple control valves and external air sources. This enables the gripper to bend and release by simply modulating air pressure through the piston's movement,

reducing mechanical complexity while enhancing operational efficiency. Additionally, integrated flexible tactile sensors embedded within the gripper fingers provide real-time feedback on contact forces, enabling precise adaptive grasping. By adjusting motor control in response to sensor data, the system can handle delicate produce without damage, making it an ideal solution for modern agricultural harvesting challenges. By addressing key limitations in existing harvesting technologies, this study presents an innovative, efficient, and adaptable robotic solution, contributing to the advancement of automated agricultural harvesting.

2 | Design and Method

2.1 | Concept Design of an Intelligent, Self-Adaptive Soft Gripper System

Inspired by the intricate sensory capabilities of the human hand, this study presents the development of an untethered, intelligent, self-adaptive soft gripper system designed for precision agricultural harvesting. Our innovative design integrates flexible tactile force sensors directly into the gripper's structure, ensuring it maintains its inherent softness and flexibility (Figure 1a). As shown in Figure 1b, the proposed gripper system employs a modular architecture based on soft pneumatic actuators. The device consists of three primary modules: (1) control module—includes a microcontroller and battery for autonomous operation, (2) power module—features a motorized syringe system driven by a stepper motor, enabling precision actuation, and (3) gripper module—the soft, adaptive end effector, capable of conforming to different fruit shapes and sizes. These components are connected via rapid connectors, allowing for quick and flexible assembly and reconfiguration, typically achievable within seconds.

A standout feature of our design is the direct connection between the syringe chamber and the gripper chambers, forming a closed pneumatic system. This setup allows internal pressure modulation through the piston's reciprocating movement, eliminating the need for external air sources. This design not only simplifies the system design but also enhances operational independence, making it more efficient and practical for field applications. The highly modular design offers significant advantages over conventional robotic systems. The reconfigurability, reusability, versatility, cost-effectiveness, and robustness of the design make it an appealing solution for various applications. Additionally, the direct syringe-to-gripper connection creates a confined pressure space, allowing precise grasping control without reliance on external air sources. This seamless integration enables the system to operate untethered, enhancing its flexibility and overall functionality.

The system is further enhanced by flexible tactile force sensors embedded within the gripper fingers, enabling real-time force detection and adaptive grasping control. This intelligent, self-adaptive gripper system, with its advanced modular design and integrated tactile sensing, represents a significant advancement in agricultural robotics. It offers a practical, efficient, and scalable solution to address modern harvesting challenges, paving

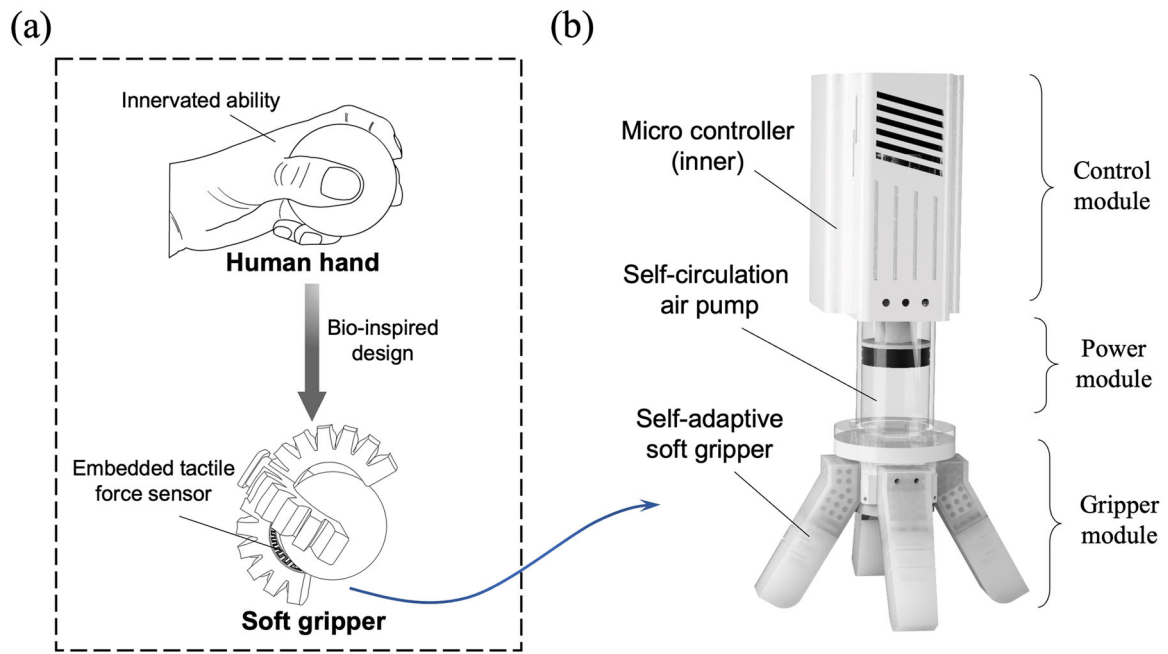


FIGURE 1 | Untethered self-adaptive soft gripper system design and its agricultural applications. (a) Human hand-inspired soft gripper, designed to replicate human dexterity, featuring embedded tactile force sensors for precise force feedback. (b) Schematic diagram illustrating the cohesive integration of the soft gripper system components. [Color figure can be viewed at [wileyonlinelibrary.com](https://onlinelibrary.wiley.com/doi/10.1002/rob.70013)]

the way for more autonomous and intelligent robotic systems in agriculture.

2.2 | Untethered Control in the Soft Gripper System

During the prototyping of the soft gripper system, we identified several key design requirements to ensure successful operation: (1) The system must provide adequate flow rate and pressure to fully actuate the gripper fingers, (2) It must incorporate reversible flow control to allow flexible and controlled movement, and (3) It must modulate internal pressure independently, eliminating the need for external air sources. To meet these requirements, we developed a micro-motorized syringe system using a piston-driven pneumatic actuation method. This design enables the adjustment of internal pressure within the syringe chamber through the piston's reciprocating motion, without reliance on external gas sources.

As illustrated in Figure 2a, the system operates via a stepper motor, which rotates a screw rod. This rotation drives a push rod via a flange nut, which in turn moves a guide holder. The guide holder's motion propels the piston within the syringe chamber, allowing for precise pressure modulation and controlled actuation of the gripper fingers. Figure 2b outlines the operating principles of the motorized syringe. Initially, the piston is at zero outlet pressure. Forward motion of the stepper motor pushes the piston forward, increasing the air pressure within the chamber. Reverse motion of the stepper motor pulls the piston backward, reducing the air pressure within the chamber. Through this reciprocating motion, the motorized syringe continuously varies the chamber's volume,

effectively modulating the pressure without external gas involvement.

According to Boyle's law, which states that the volume of an ideal gas is inversely proportional to its pressure ($PV = P_0V_0$), where P and V are the compressed air pressure and volume within the chamber, P_0 and V_0 are the initial air pressure and volume before actuation. The initial chamber volume V_0 is expressed as $V_0 = \frac{\pi(L_0D^2 + L_1d_1^2)}{4}$, where L_0 is the maximum piston stroke, D is the inner diameter of the syringe chamber, and L_1 and d_1 are the length and diameter of the syringe nozzle, respectively. After piston displacement, the chamber volume can be expressed as $V = V_0 - \Delta V = \frac{\pi[(L_0 - vt)D^2 + L_1d_1^2]}{4}$, where t is the running time of the piston, and v is the piston speed, given by $v = nd/60$, in which n is the motor's rotation speed (rpm), and d is the screw rod lead. Thus, the compressed air pressure is determined by $P = \frac{P_0(L_0D^2 + L_1d_1^2)}{(L_0 - \frac{ndt}{60})D^2 + L_1d_1^2}$. This equation quantifies the

relationship between the piston motion, chamber volume, and air pressure, providing a basis for precise pneumatic control in the soft gripper system.

To validate this design, we conducted comprehensive mechanical performance tests on the motorized syringe system. In our experimental setup (Figure 2c), we measured the syringe's output pressure using an air pressure sensor (PSE560-01) while varying the stepper motor speed across its entire operational range. Figure 2d illustrates that the syringe's output pressure increases nonlinearly with piston push time at a 250 rpm forward rotation of the stepper motor, peaking when the piston reaches its maximum stroke. Theoretical predictions closely align with experimental data, confirming the accuracy of our model in predicting syringe output pressure during piston propulsion. Figure 2e further explores the relationship between

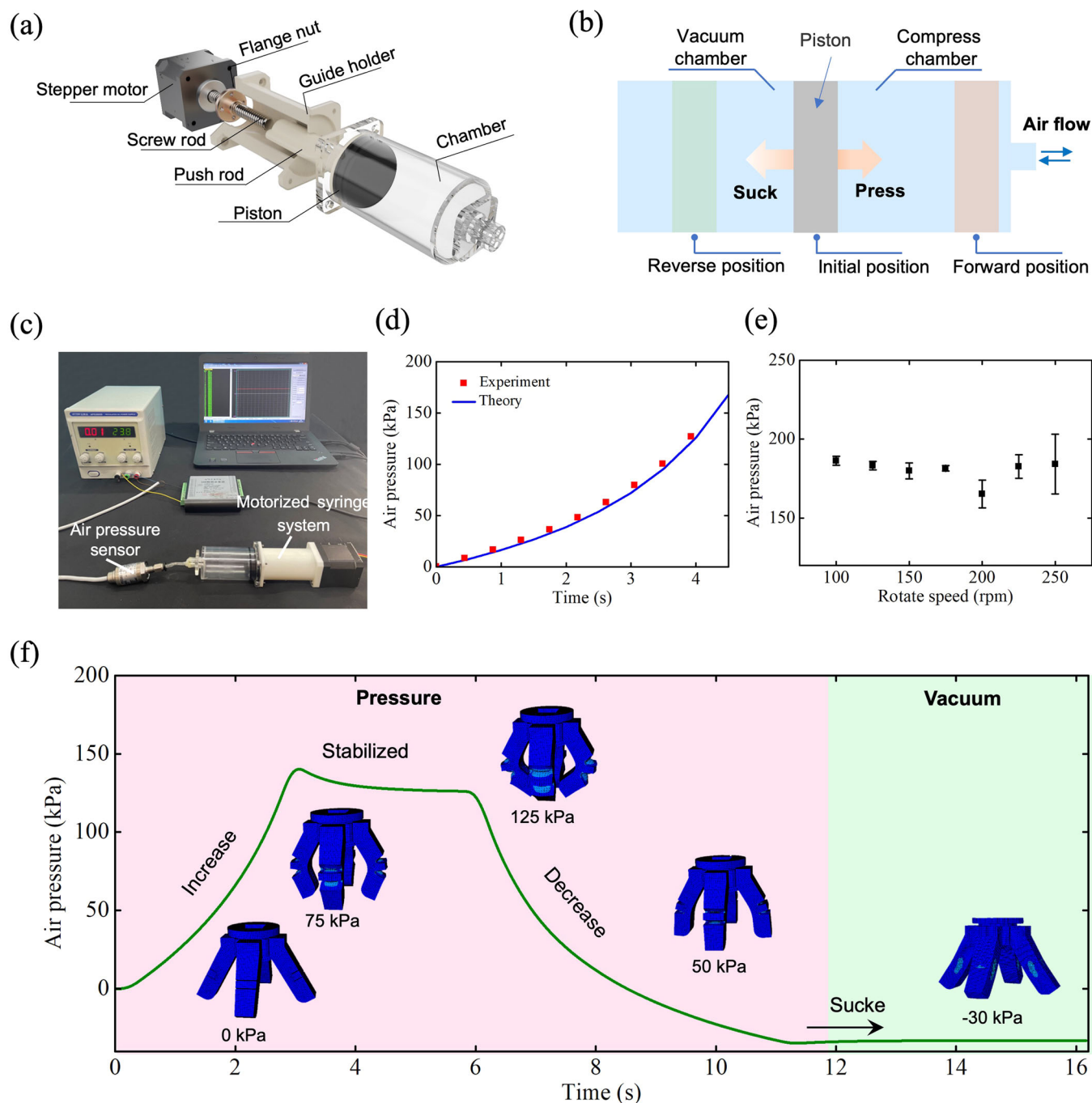


FIGURE 2 | Design and operational mechanics of the motorized syringe. (a) Schematic diagram of the motorized syringe, featuring an integrated stepper motor that drives the axial movement of the syringe piston, enabling precise pressure control. (b) Illustration of the operating principle, detailing how piston movement generates positive and negative pressures for actuation. (c) Experimental setup used to measure the syringe's outlet pressure. (d) Relationship between outlet pressure and piston running time at a stepper motor speed of 250 rpm, showing nonlinear pressure variation. (e) Dependence of peak outlet pressure on motor speed, demonstrating pressure stability across different speeds. (f) Full-range output pressure variation, illustrating how the syringe pressure increases as the piston moves forward, stabilizes at peak position, and decreases upon reversal, eventually reaching negative pressure as the piston moves beyond its initial position. [Color figure can be viewed at [wileyonlinelibrary.com](https://onlinelibrary.wiley.com/doi/10.1002/rb.20013)]

syringe peak pressure and motor rotation speed. At 100 rpm, the syringe achieves a peak pressure of 185 kPa, which slightly decreases as motor speed increases. This confirms that the syringe can generate sufficient pressure to actuate the soft gripper. However, at higher motor speeds (e.g., 250 rpm), significant pressure fluctuations are observed. The most stable operation with minimal fluctuation occurred at 175 rpm,

suggesting this speed as the optimal setting for consistent performance.

Figure 2f illustrates the full-range output pressure variation of the syringe, transitioning from positive to negative pressure at 250 rpm. As the piston moves forward, the pressure increases rapidly, then stabilizes as the motor maintains torque to hold

the piston in position. When the motor reverses, the pressure swiftly decreases, reaching a minimum of -30 kPa. Numerical simulations of gripper deformation reveal that the fingers bend progressively as pressure increases, achieving maximum bending at peak pressure. As the pressure decreases, the fingers rapidly release, and during the negative pressure phase, they bend in the opposite direction, expanding the gripper's grasping space for improved adaptability. Supporting Information S3: Table S1 provides a comparison between the motorized syringe and various miniaturized pneumatic pumps, demonstrating that motorized syringes offer superior untethered performance for soft robotic applications.

2.3 | Integration of the Intelligent Adaptive Soft Gripper

The adaptive soft gripper is an untethered, pneumatically driven device designed for effective spherical power grasping, ensuring secure form-closure around fruits. This gripper integrates flexible membrane-type sensors, enabling tactile pressure monitoring without compromising its inherent soft functionality. These sensors allow for the detection of both the tactile pressure during grasping and any frictional motion of the object within the gripper. This capability is crucial for providing feedback signals to adjust grasping forces dynamically, thereby preventing potential dropping of the object.

Based on the shape and mechanical properties of apples, we designed a two-jointed soft-rigid hybrid gripper with variable-chamber actuation that mimics the biomechanics of human fingers. As illustrated in Figure 3a, the gripper adopts a symmetric four-finger layout optimized for apple handling, with each finger angled at 30° relative to the palm plane to promote a natural wrapping motion. To enable contact detection and real-

time tactile feedback, each finger integrates an embedded flexible sensor, mimicking the sensory function of human skin.

During grasping, apples tend to settle naturally against the fingers due to gravity, forming a conical wrap configuration that enhances both stability and coverage. Each finger consists of two articulated segments, joined by a chambered structure containing three variable-size pneumatic chambers. This configuration enables the fingers to bend in a nonuniform, human-like manner, allowing better conformance to the apple's curved surface, as shown in Figure 3b,c.

To enhance grip strength and fingertip support, a rigid skeletal insert is embedded at the base of each finger. Figure 3d,e depict the gripper's bending deformation and its apple-holding state, respectively. Detailed geometric parameters of the gripper are provided in Supporting Information S3: Figure S1 and Table S2, and the fabrication process is illustrated in Supporting Information S3: Figure S2.

The electropneumatic control system of our self-adaptive soft gripper is outlined in Figure 4, which illustrates both the composition and the connection methodology of the system. At the heart of the control system is an Arduino Uno board, which is equipped with a Bluetooth module. This setup facilitates wireless communication, allowing the board to receive signals from a remote control. Once these signals are received, they are processed in accordance with a pre-programmed control algorithm. Based on this processing, the Arduino Uno then generates control commands for the motor drive module. This module is responsible for manipulating the stepper motor (42BYGH48), thereby regulating the operation of the motorized syringe system.

A critical feature of this system is the feedback loop provided by tactile force sensors during the grasping process as shown in

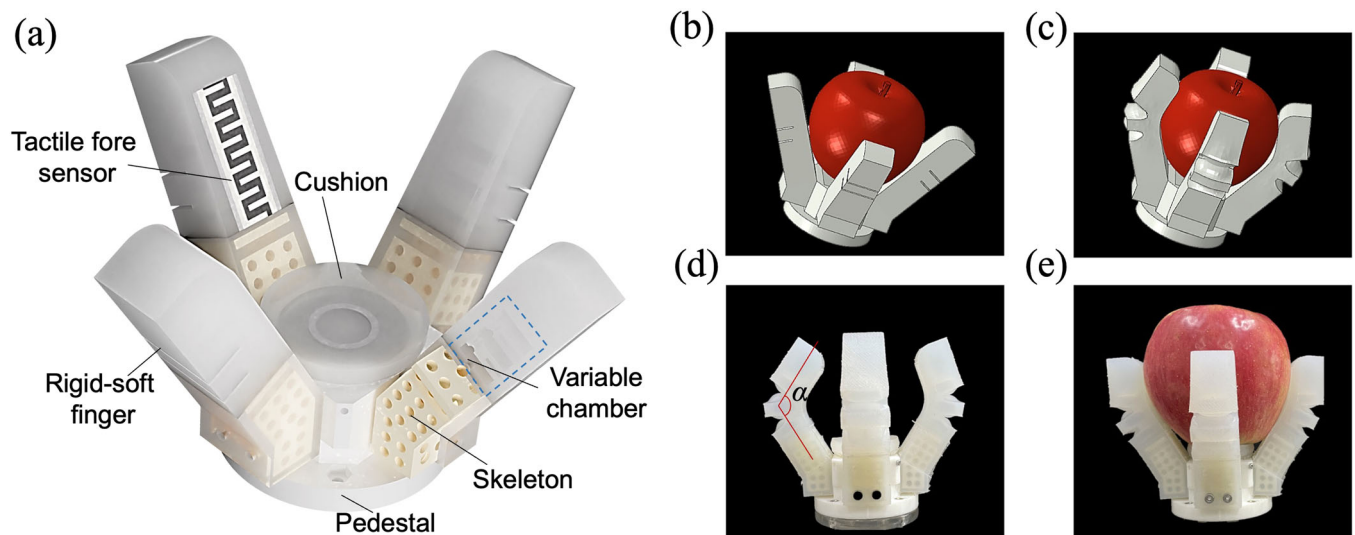


FIGURE 3 | Sensory-integrated design and functional demonstration of the self-adaptive soft-rigid gripper. (a) Schematic of the overall gripper structure, featuring a center-symmetric four-finger configuration. (b) Initial, open state of the gripper before grasping. (c) Grasping state during apple picking, illustrating conformal wrapping. (d) Illustration of the variable chamber structure, which enables biomimetic joint motion and human-like grasping postures. (e) Demonstration of effective grasping, showing the gripper securely and gently enclosing the apple. [Color figure can be viewed at [wileyonlinelibrary.com](https://onlinelibrary.wiley.com/doi/10.1002/rob.70013)]

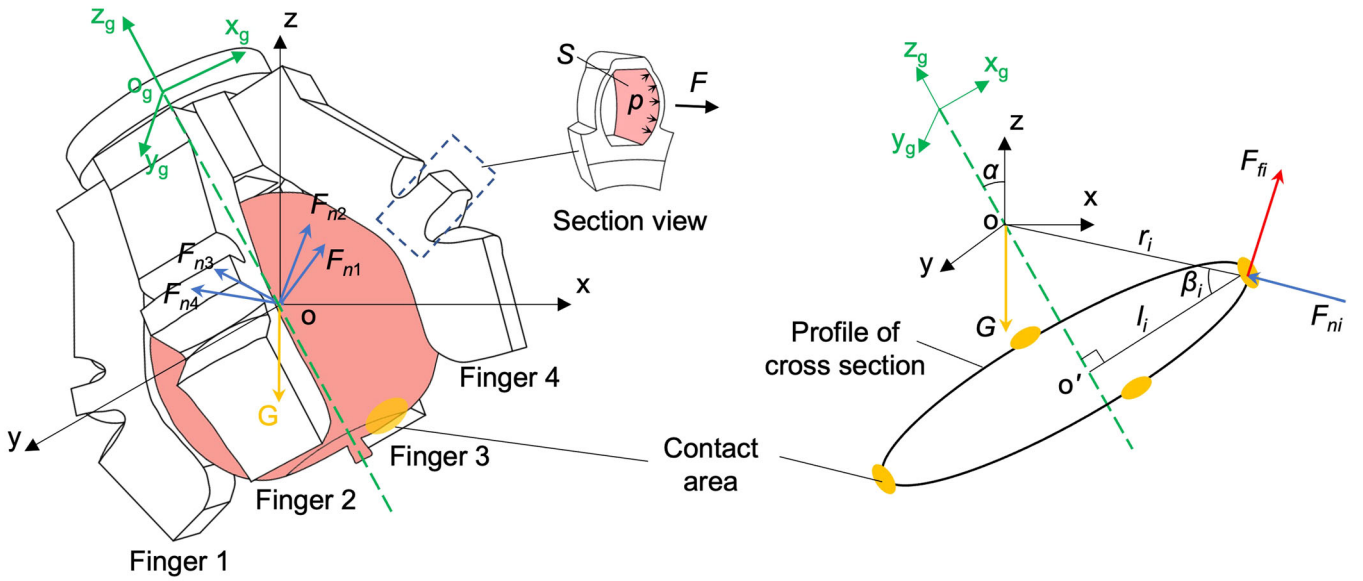


FIGURE 5 | Grasping force analysis of the soft gripper. Schematic of the theoretical model, illustrating the grasping force analysis framework for the soft gripper. [Color figure can be viewed at wileyonlinelibrary.com]

the contact position coordination coefficient (c_i), which considers the distance l_i from the contact point to the z -axis and the distance r_i from the apple's center of gravity. The normal pressure exerted by each finger, F_{ni} , can be expressed as:

$$F_{ni} = c_i K p S, i = 1, 2, 3, 4. \quad (2)$$

As pressure is applied, the chamber expands outward in an arc shape (Fig. S4). Assuming the end face deforms into a spherical shape, and neglecting wall thickness, the area after expansion is:

$$S = 2\lambda r^2 \arcsin \frac{h}{2r}, \quad (3)$$

where r is the spherical radius after chamber expansion, δ is the expansion height

$$\begin{cases} r = \frac{\delta}{2} + \frac{h^2}{8\delta} \\ \delta = \left(\frac{L}{\theta} + \frac{h}{2} + d \right) \tan \frac{\theta}{2N} - \frac{l}{2} \end{cases} \quad (4)$$

where N is the number of chambers and λ is the deformation correction factor.

From force balance, the relationship between the friction force and apple weight is derived as:

$$G = \cos \alpha \sum_{i=1}^4 c_i K p S (\sin \beta_i + \mu \cos \beta_i), \quad (5)$$

where β_i is the angle between the normal pressure of the gripper finger and the surface defined by the coordinates $x_g y_g$, and $\beta_i = \arccos \frac{l_i}{r_i}$. This analysis shows that grasping force is controlled by adjusting the air pressure $p(n, t)$ in the gripper

chamber. By modifying the motor speed (n) and pulse time (t), the gripper adapts to apples of different weights.

To evaluate the grasping performance of the two-jointed soft-rigid hybrid gripper, a series of experiments were conducted using a six-axis force/torque sensor (SRI-V-171120-A M3703B SN2704) to measure the applied forces and torques during operation. As illustrated in Figure 6a, the grasping force was measured by positioning the force sensor beneath a finger. The results showed that the gripping force increased steadily as the piston advanced, reaching a peak value of 4 N under steady-state conditions.

Figure 6b presents the results of a grasping speed experiment. In this setup, the gripper was fixed horizontally, and two reflective markers were attached to each fingertip to track their relative movements. A 3D motion capture system (NDI) was used to record the spatial trajectories of the fingertips. As the piston progressed, the fingers bent and conformed to the target geometry. Once the bending angle stabilized, it indicated a successful and secure grasp of the object. The total grasping time was recorded as 6.75 s, corresponding to an actuation frequency of 0.15 Hz. These results suggest that grasping speed is primarily governed by piston advancement, which can be optimized by increasing motor speed or adjusting the screw pitch to enhance operational efficiency in real-world applications.

To assess the pulling force and torque during fruit detachment, a 3D-printed apple model (80 mm diameter) was affixed to the force sensor. The gripper was actuated to twist and pull the model, simulating typical picking conditions. As shown in Figure 6c,d, the gripper achieved a maximum torque of 0.43 N·m, a pulling force of 8.53 N, and a pushing force of 40.1 N. These values confirm that the gripper generates sufficient mechanical force to detach fruit from branches without causing damage, validating its suitability for delicate agricultural tasks.

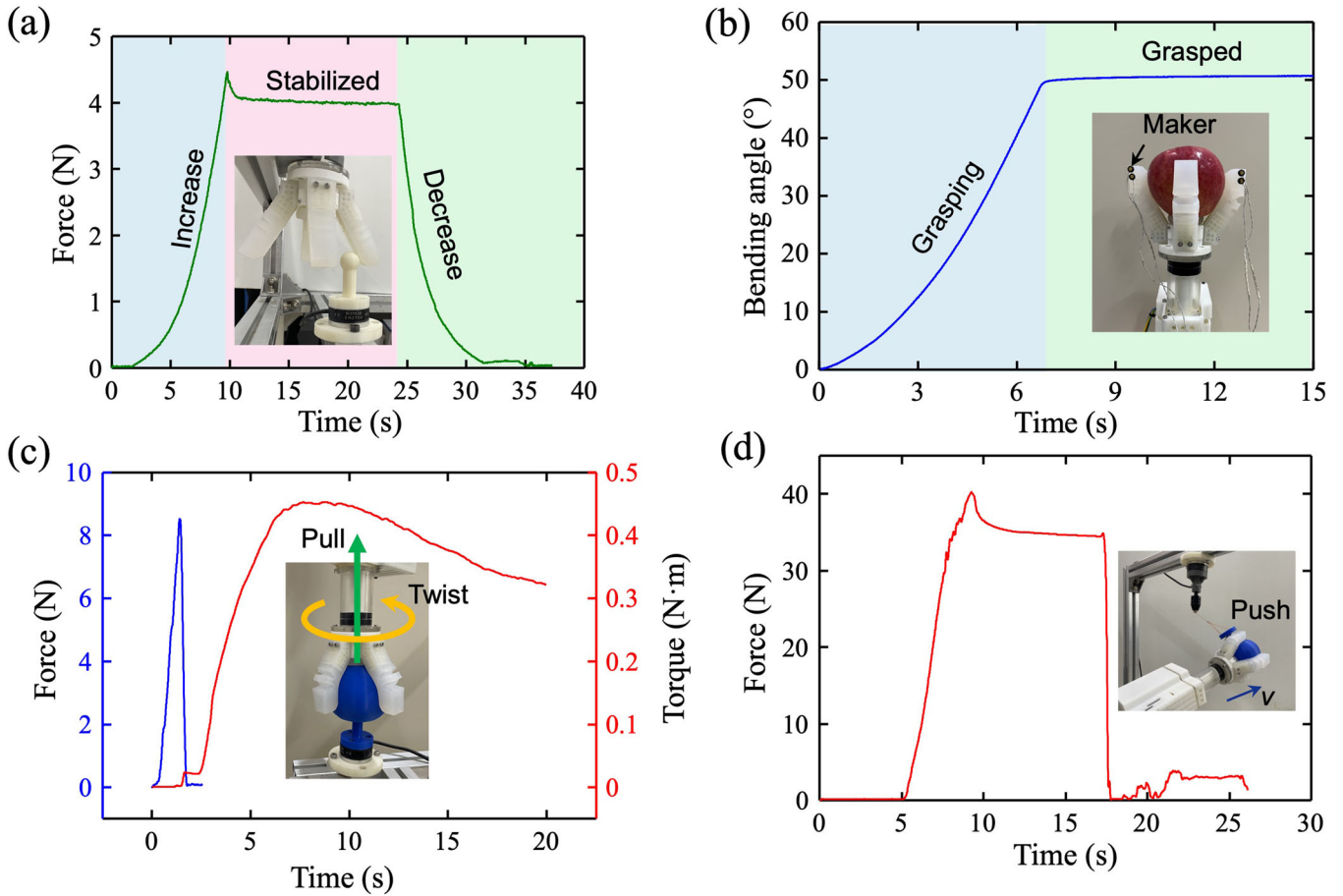


FIGURE 6 | Mechanical performance evaluation of the soft-rigid hybrid gripper. (a) Experimental setup for quantifying grasping force using a six-axis force/torque sensor placed beneath the gripper finger. (b) Grasping speed analysis using 3D motion capture, illustrating fingertip trajectory and deformation during the grasping process. (c) Measurement of pulling force and torque during simulated fruit detachment using a 3D-printed apple model mounted on the force sensor. (d) Evaluation of the lateral (pushing) force required to dislodge the apple, simulating side-loading conditions during harvesting. [Color figure can be viewed at [wileyonlinelibrary.com](https://onlinelibrary.wiley.com)]

3.2 | Soft Gripper Mechanics and Functionality

The actuation of the soft gripper fingers is accomplished via the motorized syringe system. The bending angle and output force of each finger are determined by the air pressure in its chamber, which in turn is governed by the stroke of the motorized syringe's piston. This stroke is controlled by the rotational time of the stepper motor at a specific speed. Thus, the rotation time of the stepper motor is a key factor affecting the air pressure, and consequently, the finger's bending angle and output force.

As illustrated in Figure 7b, we observe the gripper's posture at different times during the downward movement of the syringe's piston and the forward rotation of the stepper motor. The bending angle achieved by the gripper is dependent on the rotation time of the stepper motor, illustrating the relationship between motor control and gripper movement. The increase in air pressure causes progressive bending deformation of the finger. Figure 6c demonstrates the gripper's ability to grasp apples of various sizes, emphasizing the system's adaptability and responsiveness to varying physical characteristics of the fruits. To test the system's robustness, we applied an external perturbation force when the motor ceased rotating, and the air pressure remained constant. The running time of the motor (t_0)

was recorded, representing the minimum pressure needed for stable grasping. The embedded flexible tactile sensors (SF15-4) in the gripper fingers provide feedback on contact forces, enabling size recognition and adaptive grasping. Figure 7a,c detail the complete adaptive grasping process, including contact, sliding, overloading, holding, and releasing an 86 mm diameter, 304 g apple, demonstrating the gripper's versatility and precision. A universal testing machine was used to determine the threshold for apple damage, identified as pressures exceeding 25 N, as shown in Supporting Information S3: Figure S5.

3.3 | Size Recognition

The gripper's grasping posture changes with objects of varying sizes. This posture, once contact is made, remains invariant during the power grasp, meaning that the object size dictates the gripper's pose, and vice versa. For example, when grasping a sphere, the size d can be calculated as $d = 2r + w = 2l\theta + w$, where l is the finger length, θ is the envelope angle, and w is the palm width. The size recognition relative error and rate are defined as $e_{\text{size}} = \frac{\pi \sum_{i=1}^n |d - d_0|}{nd_0}$ and $\rho_{\text{size}} = (1 - e_{\text{size}}) \times 100\%$, respectively. Here, d_0 is the actual size of the object sphere. Tests on

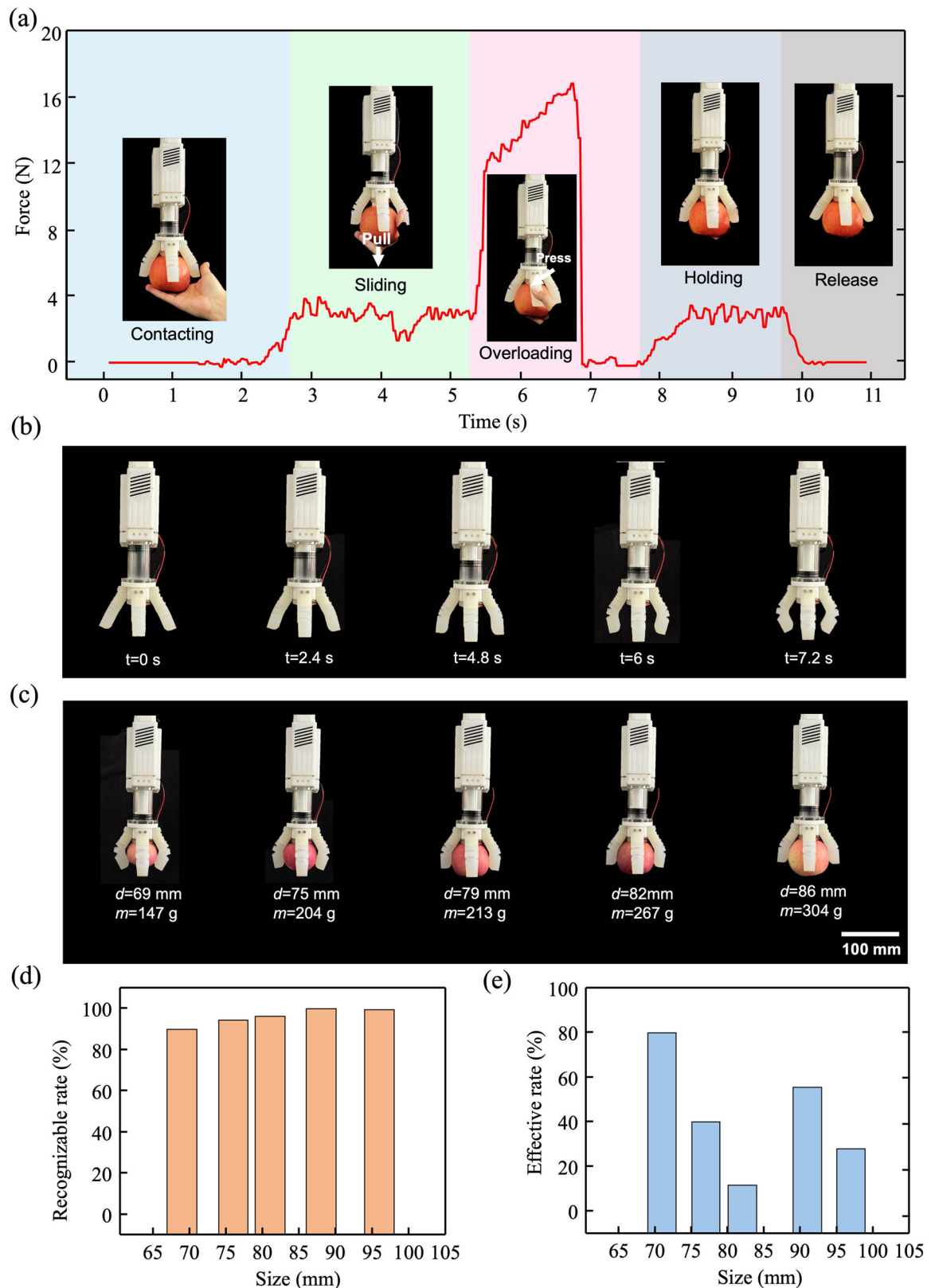


FIGURE 7 | Experimental demonstrations of the untethered self-adaptive soft gripper system. (a) The entire adaptive grasping sequence executed by the untethered soft gripper. (b) The bending deformation of the gripper was activated by the motorized syringe system. (c) Photograph highlights the gripper's capability to grasp apples of different sizes and weights. (d) Data on the size identification rates for apples with varying diameters, demonstrating the accuracy and effectiveness of the gripper's size recognition ability. (e) The efficiency improvement rate achieved through adaptive grasping. The data illustrates the enhanced performance of the gripper when utilizing its adaptive capabilities, signifying an important advancement in automated fruit handling. [Color figure can be viewed at [wileyonlinelibrary.com](https://onlinelibrary.wiley.com/doi/10.1002/rob.70013)]

TABLE 1 | Algorithm of adaptive grasping of the soft gripper system.

Algorithm 1: Adaptive Grasping Workflow	
1	while $F_n = 0$ do
	Recognizing dimension:
2	if $F_n < F_{\text{contact}}$ and $L_{\text{piston}} < L_{\text{max}}$ then
3	Submit signal to step motor to execute grasping motion;
	Record the current piston position and calculate the target object size;
4	end if
5	
6	while $F_{\text{grasp}} \geq F_{\text{contact}}$ and $L_{\text{min}} < L_{\text{piston}} < L_{\text{max}}$ do
	Adaptive grasping:
7	if $F_{\text{grasp}} \leq F_{\text{min}}$ then
8	Submit signal to step motor to execute grasping motion quickly;
	if $F_{\text{grasp}} \geq F_{\text{max}}$ then
9	Submit signal to step motor to execute release motion quickly;
10	if $F_{\text{min}} \leq F_{\text{grasp}} \leq F_{\text{max}}$ then
	Keep grasping motion;
11	end if
12	
13	
14	end while
15	end while

Note: F_{contact} is the discriminative force that decides whether the object is in contact with the gripper (0.35 N), F_{grasp} is the grasping force, F_{min} is the minimum force that can hold the object, F_{max} is the threshold force that can damage the apple (25 N), L_{piston} is the initial displacement of the piston, L_{min} and L_{max} are the limiting positions of piston for counterclockwise and clockwise rotations of the stepper motor.

apples of diameters ranging from 60 to 100 mm demonstrated that the size recognition rate is significantly higher for objects, indicating the gripper's effectiveness for this size range (Figure 7d and (Table 1)).

3.4 | Adaptive Grasping

Experiments conducted following Algorithm 1 evaluated the soft gripper's efficiency in adaptive grasping. The testing process began with minimal grasping force, followed by incremental force adjustments until a stable and secure grasp was achieved. The effectiveness of adaptive grasping (e_{grasp}) was quantified using the relative error, defined as $e_{\text{grasp}} = \frac{\pi \sum_{i=1}^n (t_c - d_0)}{nt_0}$, where t_0 is the piston's running time without the adaptive strategy, t_c is the time under adaptive control, and n is the number of samples. The results showed relative errors ranging from 0.021 to 0.167 for apples of different diameters, confirming the effectiveness of the adaptive grasping strategy in achieving precise and efficient grasping. To further assess performance, we compared grasping success

TABLE 2 | Success rate of grasping spherical fruits.

No.	Diameter d/mm	Mass m/g	Success rate/%	
			No adaptive control	Adaptive control
1	69	155	55.6	100
2	76	195	71.5	100
3	81	253	89.7	100
4	88	295	64.5	100
5	96	336	69.7	89.1

rates with and without adaptive strategies (Table 2). The efficiency improvement rate ρ_0 was calculated as $\rho_0 = \left(\frac{\lambda_c - \lambda_0}{\lambda_0} \right) \times 100\%$, where λ_0 is the success rate of multiple grasping attempts without adaptive strategies, and λ_c is the success rate using adaptive strategies. Figure 7e highlights the efficiency improvement, demonstrating that adaptive grasping significantly increases the success rate in automated apple picking. This advancement is crucial for enhancing the reliability and effectiveness of agricultural robotics in real-world applications.

4 | Demonstration of the Soft Adaptive Gripper System for Apple Harvesting

To assess the practicality and efficiency of the apple harvesting system, we first conducted laboratory-based picking tests using a controlled test platform to simulate the apple picking process. Following this, we performed field trials in a commercial apple orchard to evaluate the system's real-world performance under natural conditions.

4.1 | Apple Picking Test Trials in the Laboratory

To evaluate the performance of the self-adaptive apple harvesting system, we first conducted laboratory-based trials under controlled conditions. As illustrated in Figure 8a, the soft adaptive gripper system was mounted on a 6-DOF robotic arm, which was integrated with a ground mobile robot. The robotic arm's vision system enabled precise fruit localization, allowing the robot to navigate toward the target apple efficiently. The self-adaptive harvesting strategy, shown in Figure 8b, employed a closed-loop control mechanism that utilized real-time tactile feedback to optimize grasping. Once the robotic arm accurately positioned the gripper, the controller activated the stepper motor, which drove the motorized syringe system to pump air into the gripper's chamber, initiating the grasping process. During grasping, embedded tactile force sensors continuously monitored the contact force between the gripper fingers and the fruit. This force feedback was transmitted to the controller, which dynamically adjusted the grip to prevent slippage or excessive force, ensuring a secure and damage-free harvest. After securing the apple, the robotic arm executed a controlled twist-and-rotate motion, effectively detaching the apple from its stem before placing it in a storage container.

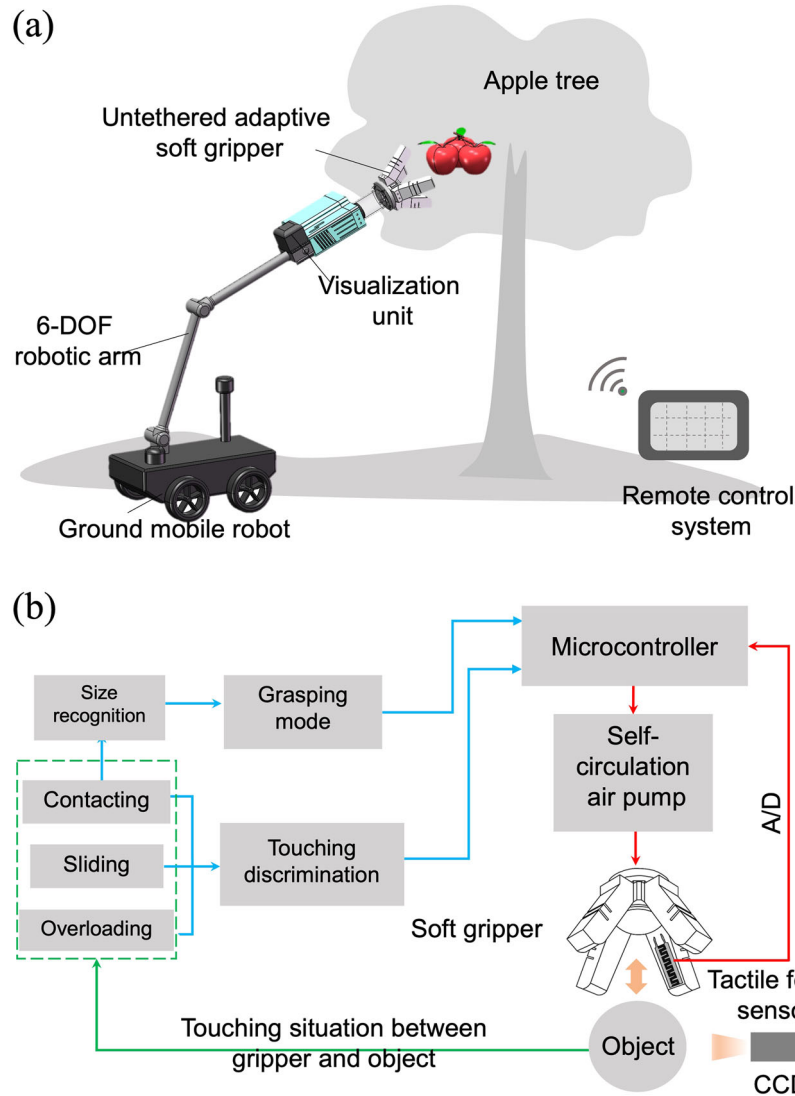


FIGURE 8 | Demonstration of the untethered self-adaptive soft gripper system in apple harvesting. (a) Schematic illustration provides a visual overview of the apple harvesting scene and the system layout. (b) Strategic approach employed by the self-adaptive soft gripper system for efficient apple harvesting. It outlines the sequence of actions and decision-making processes involved in the system's operation, from detection to grasping. [Color figure can be viewed at [wileyonlinelibrary.com](https://onlinelibrary.wiley.com/doi/10.1002/rob.20013)]

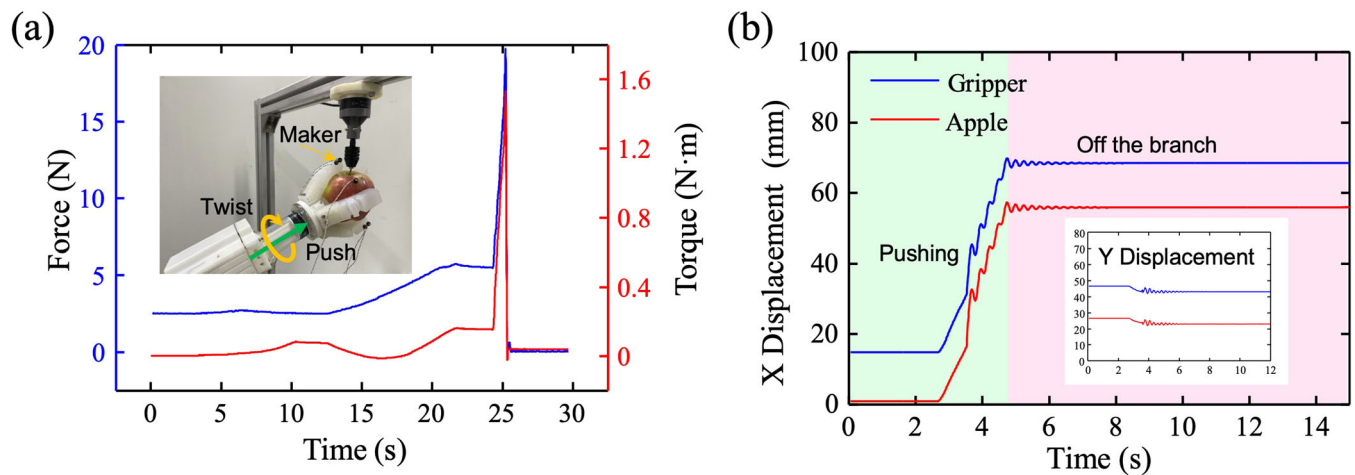


FIGURE 9 | Dynamic performance of the gripper during a simulated picking task. (a) Force measurement during the simulated apple detachment process, highlighting a transient shock force of 20 N at the moment of stem breakage. (b) Time-resolved displacement data showing minimal relative motion between the gripper and the apple, confirming stable grasp under dynamic loading. [Color figure can be viewed at [wileyonlinelibrary.com](https://onlinelibrary.wiley.com/doi/10.1002/rob.20013)]

To evaluate the gripper's ability to securely hold and detach apples, a series of dynamic loading experiments were performed to simulate real-world picking conditions. In the first test, an apple was affixed beneath a six-axis force/torque sensor, and reflective markers were placed on both the apple and the gripper to monitor their relative positions. The gripper twisted and pulled the apple until it detached from the stem, during which both forces and torques were continuously recorded.

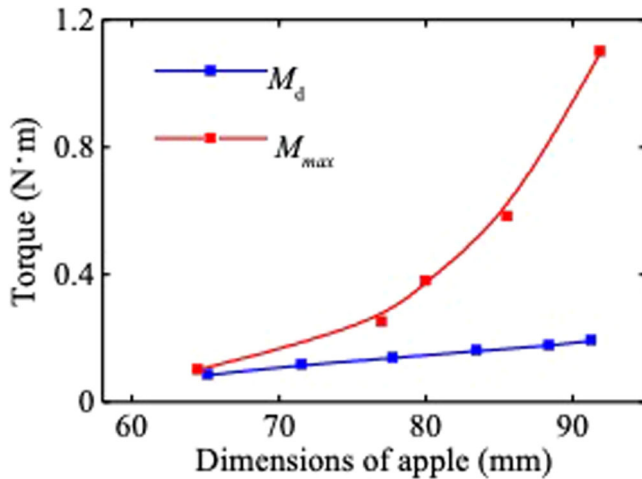


FIGURE 10 | Twisting torque analysis for apple stem detachment. Twisting torque required (M_d) to detach apples of varying sizes and the maximum torque (M_{max}) generated by the gripper. The results indicate that M_{max} consistently exceeds M_d , validating the gripper's effectiveness for apple harvesting across a range of diameters. [Color figure can be viewed at [wileyonlinelibrary.com](https://onlinelibrary.wiley.com)] [Color figure can be viewed at [wileyonlinelibrary.com](https://onlinelibrary.wiley.com)]

As shown in Figure 9a, the apple detachment event resulted in an instantaneous shock force of approximately 20 N. Displacement tracking data, collected via a 3D motion capture system, is shown in Figure 9b. The results confirm that the gripper maintained a stable grasp during the entire picking sequence, with minimal relative displacement between the gripper and the apple, even under dynamic conditions. This demonstrates the gripper's robust holding capacity and stability during harvesting.

To quantify the torque required for stem detachment across a range of apple sizes, we conducted additional experiments using real apples and a six-axis force sensor (SRI-M3703B) mounted at the interface between the gripper and a 6-DOF robotic arm. The gripper was actuated to grasp each apple laterally, and the arm applied a counterclockwise twisting motion until the stem broke. As shown in Figure 10, the detachment torque (M_d) ranged from 0.08 to 0.2 N·m for apples with lateral diameters between 65 and 91 mm, indicating that stem strength increases with apple size.

To ensure that the gripper could consistently exceed this detachment threshold, we also measured the maximum torque (M_{max}) it could exert. Apple models of varying diameters (64.5–91.9 mm) were 3D-printed and mounted on a six-axis sensor. The gripper was rotated counterclockwise, and the resulting torque was recorded. As shown in Figure 10, M_{max} ranged from 0.1 to 1.1 N·m, consistently surpassing the detachment torque M_d for all tested sizes. These findings confirm the gripper's capacity to effectively harvest apples of various sizes through controlled twisting and detachment.



FIGURE 11 | Field trials and demonstration of the harvesting system. (a and b) Field trials conducted in a commercial apple orchard in Northeast China. (c) Field testing scenario with a robotic platform featuring an arm equipped with a soft gripper and remote control. (d) A video frame showing the soft gripper successfully picking an apple. (e) Examples of harvest failures caused by over-dense apple distribution and grasping interference. [Color figure can be viewed at [wileyonlinelibrary.com](https://onlinelibrary.wiley.com)]

4.2 | Field Trials

Following the laboratory tests, we conducted field trials at a commercial apple orchard in Northeast China in September 2024, focusing on the Xiping No. 4 apple variety. The orchard contained short apple trees with narrow, flat crowns, standing 2.5–3 m tall, with crown diameters of 1.5–2 m. The trees were spaced 2–4 m apart, with branch clusters 30–40 cm apart, and each branch bore 7–12 apples (Figure 11a,b). The harvesting season (September–October) provided optimal conditions, including light rainfall, abundant sunlight, mild temperatures (18°C–23°C), minimal wind, and low humidity, facilitating efficient robotic picking. To enhance the gripper's grasping force, we implemented a two-jointed rigid-soft combination design with variable chambers. The structural parameters and mechanical properties are detailed in the Appendix. As shown in Figure 11c, the field trials utilized a tracked ground mobile robot (HRSTEK) equipped with an untethered soft gripper mounted on a six-degree-of-freedom robotic arm (uAgent-SArm). Operators remotely controlled the system, using a camera mounted on the robotic arm to guide the picking process (Supporting Information S1 and S2: Movies 1 and 2).

During field operations, the gripper employed a lateral grasping technique, using a counterclockwise wrist rotation to detach the

apple from its stem. This method does not require precise alignment of the apple, as a slight wrist rotation is sufficient to separate the stem, ensuring high efficiency and a high success rate in picking. The entire picking process, from apple identification to final placement, is illustrated in Figure 12. First, the visual sensing unit on the mechanical arm detects and locates the apple. Once identified, the ground-moving robot navigates toward the target. The robotic arm then extends, positioning the apple within the gripper's grasping range. The system adjusts the air pressure, causing the gripper fingers to open and gently trap around the apple before securely closing. Finally, the robotic arm rotates counterclockwise, twisting and detaching the apple while maintaining a firm grip, ensuring a smooth and efficient harvesting process. For immature apples, the system employed a twist-push-pull strategy, applying force in a forward or sideways direction to facilitate separation. During the field trials, the system successfully harvested 52 apples within the robot's accessible space. The apples had diameters ranging from 78 to 87 mm and an average weight of approximately 250 g. Out of these, 42 apples were successfully picked, while 10 attempts resulted in failure, yielding a harvest efficiency of 80.7%. These results highlight the effectiveness, adaptability, and robustness of the self-adaptive soft gripper system, confirming its potential for automated fruit harvesting in real-world agricultural settings.

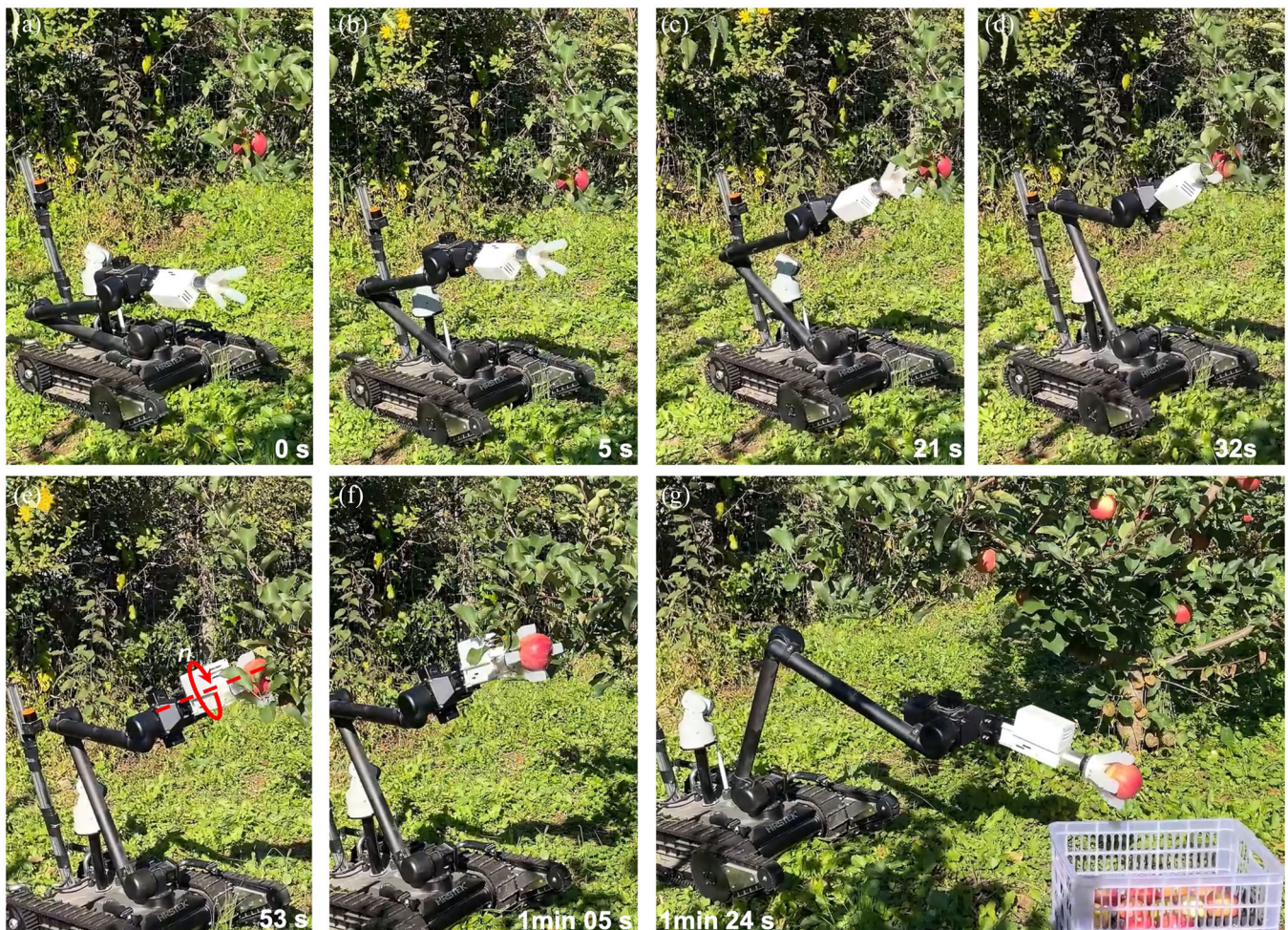


FIGURE 12 | The apple picking process with the new system. The sequence illustrates the steps from apple identification to final placement. [Color figure can be viewed at [wileyonlinelibrary.com](https://onlinelibrary.wiley.com/doi/10.1002/rob.70013)]

Figure 11d,e illustrates the successful harvesting of a sample apple during field trials. However, some failures were observed, and the underlying causes were analyzed as follows: (1) High apple density: When apples grow closely together, the gripper's fingers cannot fit through narrow gaps, making it difficult to achieve a proper grasp. (2) Obstruction by branches: Branches can interfere with the gripper, either by getting caught between the gripper and the apple or by restricting the gripper's movement, preventing effective grasping. (3) Immature apples: These apples are more firmly attached to branches, requiring higher detachment force than the gripper can provide, making separation difficult.

The harvested apples showed no signs of browning after 1 week of observation, confirming that the soft gripper applies gentle and non-damaging force during harvesting. It was demonstrated that the system required an average of 6.7 s to grasp an apple, while the entire harvesting process (excluding approach and placement time) took approximately 26 s per apple (Figure 12). Field trials confirmed that lateral grasping combined with a forward twisting motion was the most effective technique for detaching apples. The soft gripper generated sufficient force to achieve stable grasping, but further optimization is needed to enhance harvesting efficiency, making it a key focus for future system improvements.

5 | Conclusion

We have successfully developed an untethered, adaptive soft gripper system that closely mimics human tactile sensing, specifically designed for agricultural harvesting. At the core of this system is our plunger-type motorized syringe, which seamlessly integrates power supplies, control systems, and specialized end effectors into modular units. The use of fast connectors enables rapid assembly and reconfiguration, enhancing the system's flexibility and adaptability.

The motorized syringe is directly connected to the soft gripper's chamber, forming a closed internal system that allows gas exchange solely through the piston's reciprocating motion, eliminating the need for external air sources. This self-contained design simplifies the system, improving portability and ease of operation. Additionally, the integration of flexible membrane-type sensors within the gripper enables real-time size detection and adaptive grip adjustment, ensuring gentle handling of delicate produce. Laboratory and field trials demonstrated the effectiveness of the electric injector and adaptive soft gripper system. During field tests, the system successfully picked apples with diameters between 78 and 87 mm and weights of approximately 250 g, without causing any damage. The gripper completes an individual apple-picking cycle in just 6.7 s, while the total harvesting time using the mobile platform is 26 s per apple.

The untethered, adaptive soft gripper system offers significant advantages in autonomy, maneuverability, and operational efficiency. Beyond agricultural harvesting and sorting, its versatile design makes it applicable to various domains, including

soft robotics, packaging automation, and industrial handling. We believe this study represents a substantial advancement in automation and robotics, providing an efficient, adaptable, and innovative solution that unlocks new possibilities in autonomous robotic systems.

Acknowledgments

Yunwei Zhao and Xiaomin Liu acknowledge the financial support from the Department of Science and Technology of Jilin Province, China (YDZJ202401396ZYTS, YDZJ202201ZYTS624). Yi Jin, Md Shariful Islam, and Changyong (Chase) Cao are grateful for the support from National Science Foundation (ECCS-2024649), USDA-NIFA (Grant No. 2021-67021-42113), and Case Western Reserve University.

Data Availability Statement

Data sharing is not applicable to this article as no new data were created or analyzed in this study.

References

- Bac, C. W., E. J. van Henten, J. Hemming, and Y. Edan. 2014. "Harvesting Robots for High-Value Crops: State-of-the-Art Review and Challenges Ahead." *Journal of Field Robotics* 31, no. 6: 888–911.
- Bechar, A., and C. Vigneault. 2016. "Agricultural Robots for Field Operations: Concepts and Components." *Biosystems Engineering* 149: 94–111.
- Bell, M. A., B. Gorissen, K. Bertoldi, J. C. Weaver, and R. J. Wood. 2022. "A Modular and Self-Contained Fluidic Engine for Soft Actuators." *Advanced Intelligent Systems* 4, no. 1: 2100094. <https://doi.org/10.1002/aisy.202100094>.
- Blanes, C., M. Mellado, C. Ortiz, and A. Valera. 2011. "Review. Technologies for Robot Grippers in Pick and Place Operations for Fresh Fruits and Vegetables." *Spanish Journal of Agricultural Research* 9, no. 4: 1130–1141.
- Cao, C., and X. Zhao. 2013. "Tunable Stiffness of Electrorheological Elastomers by Designing Mesosstructures." *Applied Physics Letters* 103, no. 4: 041901. <https://doi.org/10.1063/1.4816287>.
- Chen, F., Z. Song, S. Chen, G. Gu, and X. Zhu. 2023. "Morphological Design for Pneumatic Soft Actuators and Robots With Desired Deformation Behavior." *IEEE Transactions on Robotics* 39, no. 6: 4408–4428.
- Chen, S., Y. Pang, H. Yuan, X. Tan, and C. Cao. 2020. "Smart Soft Actuators and Grippers Enabled by Self-Powered Tribo-Skins." *Advanced Materials Technologies* 5, no. 4: 1901075. <https://doi.org/10.1002/admt.201901075>.
- Chen, Y., Z. Gao, F. Zhang, Z. Wen, and X. Sun. 2022. "Recent Progress in Self-Powered Multifunctional E-Skin for Advanced Applications." *Exploration* 2, no. 1: 20210112. <https://doi.org/10.1002/EXP.20210112>.
- Chen, Y., S. Guo, C. Li, H. Yang, and L. Hao. 2018. "Size Recognition and Adaptive Grasping Using an Integration of Actuating and Sensing Soft Pneumatic Gripper." *Robotics and Autonomous Systems* 104: 14–24.
- Dahiya, R., N. Yogeswaran, F. Liu, et al. 2019. "Large-Area Soft e-Skin: The Challenges Beyond Sensor Designs." *Proceedings of the IEEE* 107, no. 10: 2016–2033.
- Davidson, J., S. Bhusal, C. Mo, M. Karkee, and Q. Zhang. 2020. "Robotic Manipulation for Specialty Crop Harvesting: A Review of Manipulator and End-Effector Technologies." *Global Journal of Agricultural and Allied Sciences* 2, no. 1: 25–41.
- Elfferich, J. F., D. Dodou, and C. D. Santana. 2022. "Soft Robotic Grippers for Crop Handling or Harvesting: A Review." *IEEE Access* 10: 75428–75443.

- Feng, Q. 2021. "End-Effector Technologies." In *Fundamentals of Agricultural and Field Robotics*, 191–212. https://doi.org/10.1007/978-3-030-70400-1_8.
- Goulart, R., D. Jarvis, and K. B. Walsh. 2023. "Evaluation of End Effectors for Robotic Harvesting of Mango Fruit." *Sustainability* 15, no. 8: 6769.
- Hemming, J., B. A. J. van Tuijl, W. Gauchel, and E. Wais. 2016. "Field Test of Different End-Effectors for Robotic Harvesting of Sweet-Pepper." *Acta Horticulturae* 1130: 567–574.
- Hughes, J., U. Culha, F. Giardina, F. Guenther, A. Rosendo, and F. Iida. 2016. "Soft Manipulators and Grippers: A Review." *Frontiers in Robotics and AI* 3: 69. <https://doi.org/10.3389/frobt.2016.00069>.
- Jia, W., Y. Zhang, J. Lian, Y. Zheng, D. Zhao, and C. Li. 2020. "Apple Harvesting Robot Under Information Technology: A Review." *International Journal of Advanced Robotic Systems* 17, no. 3: 172988142092531. <https://doi.org/10.1177/1729881420925310>.
- Karimi, M. A., V. Alizadehyazdi, H. M. Jaeger, and M. Spenko. 2022. "A Self-Reconfigurable Variable-Stiffness Soft Robot Based on Boundary-Constrained Modular Units." *IEEE Transactions on Robotics* 38, no. 2: 810–821.
- Li, H., J. Yao, C. Wei, P. Zhou, Y. Xu, and Y. Zhao. 2021. "An Untethered Soft Robotic Gripper With High Payload-to-Weight Ratio." *Mechanism and Machine Theory* 158: 104226.
- Li, J., L. Liu, Y. Liu, and J. Leng. 2019. "Dielectric Elastomer Spring-Roll Bending Actuators: Applications in Soft Robotics and Design." *Soft Robotics* 6, no. 1: 69–81.
- Li, S., H. Zhao, and R. F. Shepherd. 2017. "Flexible and Stretchable Sensors for Fluidic Elastomer Actuated Soft Robots." *MRS Bulletin* 42, no. 2: 138–142.
- Liu, X., Y. Zhao, D. Geng, S. Chen, X. Tan, and C. Cao. 2021. "Soft Humanoid Hands With Large Grasping Force Enabled by Flexible Hybrid Pneumatic Actuators." *Soft Robotics* 8, no. 2: 175–185.
- Liu, X., M. Song, Y. Fang, Y. Zhao, and C. Cao. 2022. "Worm-Inspired Soft Robots Enable Adaptable Pipeline and Tunnel Inspection." *Advanced Intelligent Systems* 4, no.1: 2100128.
- Morar, C. A., I. A. Doroftei, I. Doroftei, and M. G. Hagan. 2020. "Robotic Applications on Agricultural Industry. A Review." *IOP Conference Series: Materials Science and Engineering* 997, no. 1: 012081.
- Navas, E., R. Fernández, D. Sepúlveda, M. Armada, and P. Gonzalez-de-Santos. 2021a. "Soft Grippers for Automatic Crop Harvesting: A Review." *Sensors* 21, no. 8: 2689. <https://doi.org/10.3390/s21082689>.
- Navas, E., R. Fernandez, D. Sepulveda, M. Armada, and P. Gonzalez-de-Santos. 2021b. "Soft Gripper for Robotic Harvesting in Precision Agriculture Applications." *IEEE International Conference on Autonomous Robot Systems and Competitions (ICARSC)* 2021: 167–172.
- Rogers, J. A., T. Someya, and Y. Huang. 2010. "Materials and Mechanics for Stretchable Electronics." *Science* 327, no. 5973: 1603–1607.
- Shintake, J., V. Cacucciolo, D. Floreano, and H. Shea. 2018. "Soft Robotic Grippers." *Advanced Materials* 30, no. 29: 1707035. <https://doi.org/10.1002/adma.201707035>.
- Silwal, A., J. R. Davidson, M. Karkee, C. Mo, Q. Zhang, and K. Lewis. 2017. "Design, Integration, and Field Evaluation of a Robotic Apple Harvester." *Journal of Field Robotics* 34, no. 6: 1140–1159. <https://doi.org/10.1002/rob.21715>.
- Tinoco, V., M. F. Silva, and F. N. Santos, et al. 2021a. "An Overview of Pruning and Harvesting Manipulators." *Industrial Robot: The International Journal of Robotics Research and Application* 49, no. 4: 688–695.
- Tinoco, V., M. F. Silva, F. N. Santos, et al. 2021b. "A Review of Pruning and Harvesting Manipulators." *2021 IEEE International Conference on Autonomous Robot Systems and Competitions (ICARSC)*: 155–160.
- Vrochidou, E., V. N. Tsakalidou, I. Kalathas, T. Gkrimpizis, T. Pachidis, and V. G. Kaburlasos. 2022. "An Overview of End Effectors in Agricultural Robotic Harvesting Systems." *Agriculture (London)* 12, no. 8: 1240.
- Wang, W., and S.-H. Ahn. 2017. "Shape Memory Alloy-Based Soft Gripper With Variable Stiffness for Compliant and Effective Grasping." *Soft Robotics* 4, no. 4: 379–389.
- Yamaguchi, T., T. Kashiwagi, T. Arie, S. Akita, and K. Takei. 2019. "Human-Like Electronic Skin-Integrated Soft Robotic Hand." *Advanced Intelligent Systems* 1, no. 2: 1900018. <https://doi.org/10.1002/aisy.201900018>.
- Zhang, B., Y. Xie, J. Zhou, K. Wang, and Z. Zhang. 2020a. "State-of-the-Art Robotic Grippers, Grasping and Control Strategies, as Well as Their Applications in Agricultural Robots: A Review." *Computers and Electronics in Agriculture* 177: 105694.
- Zhang, Z., C. Igathinathane, J. Li, Y. Lu, H. Cen, and P. Flores. 2020b. "Technology Progress in Mechanical Harvest of Fresh Market Apples." *Computers and Electronics in Agriculture* 175: 105606.

Supporting Information

Additional supporting information can be found online in the Supporting Information section.